Pergamon

Int. J. Solids Structures Vol. 35, No 30, pp. 3977–3987, 1998

0020–7683/98 $19.00 + .00

PII: S0020–7683(97)00266–7

A FIBER/MATRIX/COMPOSITE MODEL WITH A COMBINED CONFOCAL ELLIPTICAL CYLINDER UNIT CELL FOR PREDICTING THE EFFECTIVE LONGITUDINAL SHEAR MODULUS

C. P. JIANG
Department of Flight Vehicle Design and Applied Mechanics, Beijing University of Aeronautics and Astronautics, Beijing 100083, P.R. China

and

Y. K. CHEUNG*
Department of Civil and Structural Engineering, The University of Hong Kong, Hong Kong

(*Received* 4 *April* 1997; *in revised form* 10 *July* 1997)

Abstract—A fiber/matrix/composite model with a combined confocal elliptical cylinder unit cell is proposed for predicting the effective longitudinal shear modulus of fiber reinforced composite materials from the constituent materials. The conformal mapping technique is applied to the model, resulting in closed form solutions which are applicable to extreme types of the inclusion phases (from voids to rigid inclusions), as well as can accommodate a full range of variations in fiber section aspect ratios (from circular fibers to ribbons). A comparison is made with other numerical and experimental results to demonstrate the superiority of the proposed model and the accuracy of the solutions. © 1998 Elsevier Science Ltd. All rights reserved.

1. INTRODUCTION

The fiber/matrix model of a combined circular cylinder is a classical and simple model for predicting the effective moduli of unidirectional fiber reinforced composite materials (Hashin, 1964; Whitney and Riley, 1966). The theoretical predictions from the model show reasonable agreement with experimental data for the tensile modulus, whereas very poor agreement is demonstrated for the longitudinal shear modulus (Whitney and Riley, 1966). The reason is that the combined circular cylinder cell does not account for the effect of the aspect ratio of the fiber section and the action of surrounding unit cells, which seem to be more sensitive in changing the value of the longitudinal shear modulus.

In recent years considerable attention has been focused on the effective moduli of composite materials as conventional materials are continuously being replaced by a variety of composite materials, and several approaches have been developed. The Mori–Tanaka method (Mori and Tanaka, 1973; Taya and Chou, 1981; Benveniste, 1985; Zhao and Weng, 1990) has many diverse applications in that it can accommodate elliptical inclusions, thereby accounting for a wide range of variations in inclusion shapes. Another method, the inclusion/matrix/composite model (Christensen and Lo, 1979; Luo and Weng, 1987; Christensen, 1993; Huang and Hu, 1995) (also referred to as the generalized self-consistent method) provides accurate predictions for extreme types of inclusions (i.e. voids and rigid inclusions), and the method also gives the correct asymptotic behavior of composites as the inclusion volume fraction approaches 1 (fully packed). The early inclusion/matrix/composite model can only accommodate cylindrical and spherical inclusions. Huang and Hu (1995) extended the model to cover the case of elliptical inclusions, which can account for a wide range of shape variations, and they addressed in detail the problem of an in-plane isotropic distribution of elliptical inclusions (the transverse moduli of the fiber reinforced composite materials). In Huang and Hu's model the unit cell is an elliptical

* Author to whom correspondence should be addressed.

inclusion and a surrounding elliptical ring matrix, which, in turn, is embedded in an infinite composite. The elliptical inclusion and ring share the coinciding major axes and the same aspect ratio (the ratio of the semiminor axis to semimajor axis), γ, which can be taken as $0 < \gamma \leqslant 1$ without loss of generality. Huang and Hu's investigation (1995) shows that the series solution for the model can guarantee the convergence for $\gamma > 0.1$. However, oscillation occurs as the number of series terms increases for $\gamma < 0.1$. Thus, the model has difficulty in accommodating ribbon shape inclusions. The reason is that for a small value of γ, a large amount of the matrix material in a unit cell of the model will aggregate around the two sharp ends of the inclusion, which would seem to be physically unreasonable.

In this paper a fiber/matrix/composite model, in which a unit cell is a combined cylinder with confocal elliptical cross sections, is proposed and the case of longitudinal shearing is addressed in detail for predicting the effective shear modulus. The new model gives a reasonable distribution of the matrix material in a unit cell for a full range of variation in γ (from ribbons to circular cylinders). Furthermore, by using the conformal mapping technique, a closed form solution for the effective longitudinal shear modulus for unidirectional fiber reinforced composite materials is obtained, which is particularly convenient for applications in engineering. Lastly a comparison with other numerical and experimental results is made to demonstrate the superiority of the proposed model and the accuracy of the solutions.

2. MODEL

The unit cell of the proposed model is a combined cylinder (a fiber embedded in a finite matrix), which, in turn, is embedded in an infinite "homogenization" composite. Figure 1 is a schematic diagram of the cross section of a unit cell. The elliptical region Ω_1 encircled by the contour L_1 represents the fiber section and the elliptical ring region Ω_2 between L_1 and L_2 represents the matrix section in the unit cell. Let λ denote the volume fraction of the fiber, then we have

$$\lambda = \frac{\Omega_1}{\Omega_1 + \Omega_2} \tag{1}$$

The two ellipses share the common foci O_1 and O_2, which is on the x-axis. Outside the L_2 is the "homogenization" composite, the moduli of which are to be determined. O_1O_2 is an imaginary cut for the convenience of analyses later. In order to determine the effective longitudinal shear modulus of the composite, a uniform longitudinal shear stress τ at infinity is applied to the composite in the direction of the x'-axis with β being the angle

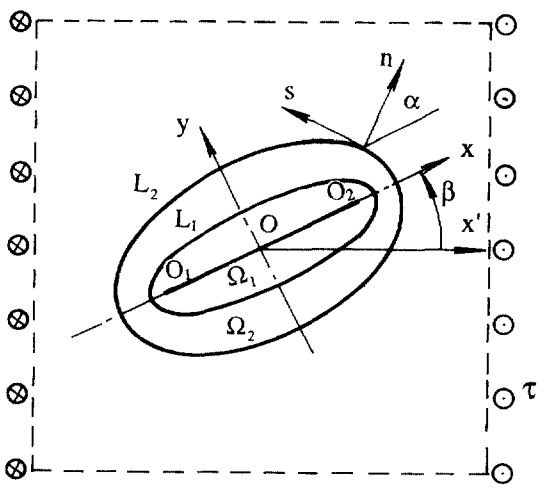

Fig. 1. Cross section of a unit cell.

made by the x-axis and x'-axis. For the convenience of describing the continuous conditions in the interfaces of the fiber/matrix and matrix/composite, the curvilinear orthogonal coordinates, n and s, which lie, respectively, along the normal and tangent of the contours L_1 or L_2, are set up with α being the angle made by the n-axis and x-axis.

Let w denote the longitudinal displacement, τ_{xz} and τ_{yz}, τ_{nz} and τ_{sz} denote the longitudinal shear stresses in the Cartesian coordinates and the curvilinear orthogonal coordinates, respectively, then the continuous conditions of the displacements and stresses on L_1 and L_2 can be expressed as

$$w_f = w_m, \quad \tau_{nzf} = \tau_{nzm} \quad \text{on } L_1 \tag{2}$$

$$w_m = w_e, \quad \tau_{nzm} = \tau_{nze} \quad \text{on } L_2 \tag{3}$$

where the subscripts f, m and e refer to the fiber, matrix and effective composite, respectively.

The stresses at infinity in the Cartesian coordinates can be expressed as

$$\tau_{xz}^{\infty} = \tau \cos\beta, \quad \tau_{yz}^{\infty} = -\tau \sin\beta \tag{4}$$

Since the shear stress components are equal in pairs there are shear stresses on the cross section of the unit cell and their resultants in the Cartesian coordinates, Q_x and Q_y, can be calculated:

$$\begin{aligned} Q_x &= \iint_{\Omega_1} \tau_{xzf}\, d\Omega + \iint_{\Omega_2} \tau_{xzm}\, d\Omega \\ Q_y &= \iint_{\Omega_1} \tau_{yzf}\, d\Omega + \iint_{\Omega_2} \tau_{yzm}\, d\Omega \end{aligned} \tag{5}$$

In the case when the fibers are uniformly dispersed and the elliptical cross sections of the fibers are randomly oriented in the transverse plane, the composite can be regarded as transversely isotropic, and the resultants of stresses of the unit cell given by eqn (5) can be taken to be average over the azimuth β. The resultants of shear stresses on the cross section of a unit cell are equivalent between two different views of the composite: one regards the composite as an overall effective medium, and the other goes into the detail of the unit cell. The equivalent condition of the shear stress in the direction of the x'-axis leads to the following equation:

$$\frac{1}{2\pi}\int_0^{2\pi} (Q_x \cos\beta - Q_y \sin\beta)\, d\beta = \tau(\Omega_1 + \Omega_2) \tag{6}$$

in terms of which, the longitudinal shear modulus of the composite can be determined.

3. ANALYSIS AND SOLUTION

It is well known that the governing equation for the longitudinal shear problem is a harmonic equation, and the longitudinal displacement w, the shear stress components τ_{xz} and τ_{yz} in the Cartesian coordinates and τ_{nz} and τ_{sz} in the curvilinear coordinates can be expressed in terms of an analytical function $f^*(z)$ (where the same symbol is used for a complex variable $z = x + iy$ and for the axial coordinate z of a unit cell, and should not be confused with each other):

$$w = \mathrm{Re} f^*(z) \tag{7}$$

$$\tau_{xz} - i\tau_{yz} = Gf^{*\prime}(z) \tag{8}$$

$$\tau_{nz} - i\tau_{sz} = G e^{i\alpha} f^{*\prime}(z) \tag{9}$$

where G is the shear modulus, the superscript prime denotes differentiation with respect to the argument, and Re denotes the real part of a function.

To solve the problem, another complex variable

$$\zeta = \xi + i\eta = \rho e^{i\theta} \tag{10}$$

is introduced, where ρ and θ are the polar coordinates in the complex ζ-plane. Making use of the conformal transformation of the z-plane onto the ζ-plane (Muskhelishivili, 1975)

$$z = \omega(\zeta) = R\left(\zeta + \frac{1}{\zeta}\right) \tag{11}$$

where R is a constant to be determined, the regions Ω_1 and Ω_2 surrounded by the imaginary cut O_1O_2, the elliptical contours L_1 and L_2 in the z-plane (Oxy-plane, Fig. 1) are mapped onto the circular ring regions Ω_1' and Ω_2' surrounded by L_0', L_1' and L_2' with radii $\rho_0 = 1$, ρ_1 and ρ_2 in the ζ-plane (Fig. 2), respectively. From this transformation, it is seen that

$$x = R\left(\rho + \frac{1}{\rho}\right)\cos\theta, \quad y = R\left(\rho - \frac{1}{\rho}\right)\sin\theta \tag{12}$$

$$a_k = R\left(\rho_k + \frac{1}{\rho_k}\right), \quad b_k = R\left(\rho_k - \frac{1}{\rho_k}\right) \tag{13}$$

where a_k and b_k are the length of the semimajor and semiminor axes, and the subscript $k = 1, 2$ refers to L_1 and L_2, respectively. Since the geometrical parameters of the fiber section, a_1 and b_1, are known, R and ρ_1 can be determined by using eqn (13). From Fig. 1, it is seen that

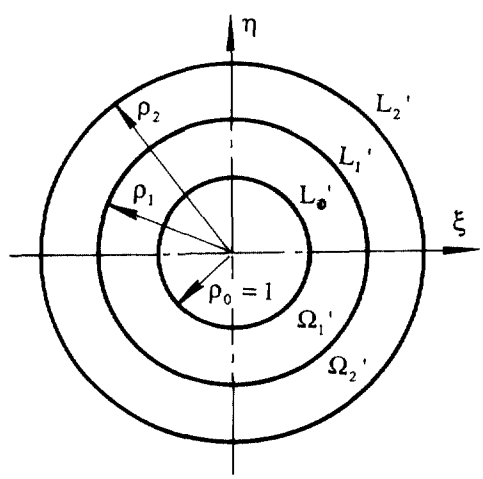

Fig. 2. Conformal mapping.

$$\Omega_1 = \pi a_1 b_1 = \pi R^2(\rho_1^2 - 1/\rho_1^2) \tag{14}$$

$$\Omega_1 + \Omega_2 = \pi a_2 b_2 = \pi R^2(\rho_2^2 - 1/\rho_2^2) \tag{15}$$

The substitution of eqns (14) and (15) into eqn (1) yields

$$\lambda = \frac{\rho_1^2 - 1/\rho_1^2}{\rho_2^2 - 1/\rho_2^2} \tag{16}$$

in terms of which, ρ_2 can be determined as the volume fraction of fibers λ is prescribed. Let

$$f(\zeta) = f^*(z) = f^*[\omega(\zeta)] \tag{17}$$

then from the chain rule for differentiation, we have

$$f^{*\prime}(z) = f'(\zeta)/\omega'(\zeta) \tag{18}$$

Applying eqn (18) and noting (Muskhelishivili, 1975) that

$$e^{i\alpha} = \frac{\zeta}{\rho} \cdot \frac{\omega'(\zeta)}{|\omega'(\zeta)|} \tag{19}$$

where $|\cdot|$ expresses the absolute value, eqns (7)–(9) become

$$w = \mathrm{Re} f(\zeta) \tag{20}$$

$$\tau_{xz}^{\infty} - i\tau_{yz}^{\infty} = G \cdot f'(\zeta)/\omega'(\zeta) \tag{21}$$

$$\tau_{nz} - i\tau_{sz} = G \cdot \frac{\zeta}{\rho} \cdot \frac{f'(\zeta)}{|\omega'(\zeta)|} \tag{22}$$

Through the above transformation, the problem under consideration (Fig. 1) has been reduced to a connection problem of the concentric circular rings in the ζ-plane (Fig. 2), which is easy to solve by using the method of power series. In the region Ω_1' in the ζ-plane, the analytical function relevant to the fiber in a unit cell, $f_1(\zeta)$, can be expanded into the Laurent series:

$$f_1(\zeta) = a^* \ln \zeta + \sum_{k=-\infty}^{\infty} a_k \zeta^k \tag{23}$$

Since the geometry of a unit cell is symmetric with respect to the x-axis and y-axis, the resultant shear stress component Q_x on the unit cell section $(\Omega_1 + \Omega_2)$ is only dependent on the shear stress at infinity τ_{xz}^{∞}, and Q_y on τ_{yz}^{∞}. For simplicity, the two cases will be dealt with separately. First let

$$\tau_{xz}^{\infty} = \tau \cos\beta, \quad \tau_{yz}^{\infty} = 0 \tag{24}$$

apparently the displacement w is symmetric with respect to the x-axis. Noting that

$$\zeta^k = \rho^k(\cos k\theta + i \sin k\theta) \tag{25}$$

from eqns (20) and (23), it can be seen that the undetermined coefficients a^* and a_k are real constants. Since O_1O_2 in the z-plane is only an imaginary cut, $\zeta = e^{i\theta}$ and $\zeta = e^{-i\theta}$ in the ζ-plane are corresponding to a same point in the z-plane, which leads to

$$f_1(e^{i\theta}) = f_1(e^{-i\theta}) \tag{26}$$

From eqn (26), it can be inferred that

$$a^* = 0, \quad a_{-k} = a_k \quad k = 0, 1, 2, \ldots \tag{27}$$

From further analyses, it is seen that the exact solution can be obtained by taking two terms ($k = -1, 1$) in the expansion (23), so the function $f_1(\zeta)$ in the region Ω_1' in the ζ-plane can be expressed as

$$f_1(\zeta) = A\left(\zeta + \frac{1}{\zeta}\right) \tag{28}$$

where A is a real constant. Substituting eqn (28) into eqns (20)–(22) and separating out the real and imaginary parts, one obtains

$$w_f = A\left(\rho + \frac{1}{\rho}\right)\cos\theta \tag{29}$$

$$\tau_{xzf} = \frac{G_f}{R}A \tag{30}$$

$$\tau_{nzf} = \frac{G_f A}{|\omega'(\zeta)|}\left(1 - \frac{1}{\rho^2}\right)\cos\theta \tag{31}$$

Similarly, in the region Ω_2' in the ζ-plane, the function $f_2(\zeta)$ relevant to the matrix in a unit cell can be expressed as

$$f_2(\zeta) = \frac{B_{-1}}{\zeta} + B_1\zeta \tag{32}$$

where B_{-1} and B_1 are real constants. The substitution of eqn (32) into eqns (20)–(22) yields

$$w_m = \left(\frac{B_{-1}}{\rho} + B_1\rho\right)\cos\theta \tag{33}$$

$$\tau_{xzm} = G_m \,\mathrm{Re}\frac{-B_{-1}/\zeta^2 + B_1}{R(1 - 1/\zeta^2)} \tag{34}$$

$$\tau_{nzm} = \frac{G_m}{|\omega'(\zeta)|}\left(B_1 - \frac{B_{-1}}{\rho^2}\right)\cos\theta \tag{35}$$

In the external region of the contour L_2' in the ζ-plane, the function $f_3(\zeta)$, which is relevant to the effective composite, can be expressed as

$$f_3(\zeta) = \frac{C_{-1}}{\zeta} + C_1\zeta \tag{36}$$

where C_{-1} and C_1 are real constants. In the same manner, w_e, τ_{xze} and τ_{nze} can be written as

$$w_e = \left(\frac{C_{-1}}{\rho} + C_1\rho\right)\cos\theta \tag{37}$$

$$\tau_{xze} = G_e \,\mathrm{Re}\frac{-C_{-1}/\zeta^2 + C_1}{R(1-1/\zeta^2)} \tag{38}$$

$$\tau_{nze} = \frac{G_e}{|\omega'(\zeta)|}\left(C_1 - \frac{C_{-1}}{\rho^2}\right)\cos\theta \tag{39}$$

where G_e is the effective longitudinal shear modulus.

Substituting eqns (29), (31), (33), (35), (37) and (39) into eqns (2), (3) and (24), six equations are obtained. Since $\tau_{yz}^{\infty} = 0$ leads to an identity, only five linear algebraic equations are independent, in terms of which, five real coefficients A, B_{-1}, B_1, C_{-1} and C_1 can be determined:

$$A = 4G_m R\tau_{xz}^{\infty} \Bigg/ \left\{\left[(G_f+G_m)\left(1+\frac{1}{\rho_2^2}\right) - (G_f-G_m)\left(\frac{1}{\rho_1^2}+\frac{\rho_1^2}{\rho_2^2}\right)\right]G_e + \left[(G_f+G_m)\left(1-\frac{1}{\rho_2^2}\right) - (G_f-G_m)\left(\frac{1}{\rho_1^2}-\frac{\rho_1^2}{\rho_2^2}\right)\right]G_m\right\} \tag{40}$$

$$B_{-1} = \left(\frac{G_f+G_m}{2G_m} - \frac{G_f-G_m}{2G_m}\rho_1^2\right)A \tag{41}$$

$$B_1 = \left(\frac{G_f+G_m}{2G_m} - \frac{G_f-G_m}{2G_m}\cdot\frac{1}{\rho_1^2}\right)A \tag{42}$$

$$C_{-1} = \left[\frac{G_f+G_m}{2G_m}(1+\rho_2^2) - \frac{G_f-G_m}{2G_m}\left(\frac{\rho_2^2}{\rho_1^2}+\rho_1^2\right)\right]A - \frac{R\tau_{xz}^{\infty}}{G_e}\rho_2^2 \tag{43}$$

$$C_1 = \frac{R\tau_{xz}^{\infty}}{G_e} \tag{44}$$

Substituting eqns (40)–(42) into eqns (30) and (34), then substituting them into the first equation of (5), one obtains

$$Q_x = \frac{2I_3G_m}{I_1G_e + I_2G_m}\cdot\tau(\Omega_1+\Omega_2)\cos\beta \tag{45}$$

where

$$I_1 = (G_m+G_f)\left(1+\frac{1}{\rho_2^2}\right) - (G_f-G_m)\left(\frac{1}{\rho_1^2}+\frac{\rho_1^2}{\rho_2^2}\right) \tag{46}$$

$$I_2 = (G_m+G_f)\left(1-\frac{1}{\rho_2^2}\right) - (G_f-G_m)\left(\frac{1}{\rho_1^2}-\frac{\rho_1^2}{\rho_2^2}\right) \tag{47}$$

$$I_3 = 2G_f\lambda + (G_m + G_f)(1-\lambda) - (G_f - G_m)\left(\frac{\rho_2^2}{\rho_1^2} - \frac{\rho_1^2}{\rho_2^2}\right)\Big/\left(\rho_2^2 - \frac{1}{\rho_2^2}\right) \tag{48}$$

Now consider another stress state at infinity:

$$\tau_{xz}^{\infty} = 0, \quad \tau_{yz}^{\infty} = -\tau \sin\beta \tag{49}$$

Apparently, in this case the displacement w is antisymmetric with respect to the x-axis. In the same manner, one can obtain

$$Q_y = -\frac{2I_6 G_m}{I_4 G_e + I_5 G_m} \cdot \tau(\Omega_1 + \Omega_2)\sin\beta \tag{50}$$

where

$$I_4 = (G_m + G_f)\left(1 - \frac{1}{\rho_2^2}\right) + (G_f - G_m)\left(\frac{1}{\rho_1^2} - \frac{\rho_1^2}{\rho_2^2}\right) \tag{51}$$

$$I_5 = (G_m + G_f)\left(1 + \frac{1}{\rho_2^2}\right) + (G_f - G_m)\left(\frac{1}{\rho_1^2} + \frac{\rho_1^2}{\rho_2^2}\right) \tag{52}$$

$$I_6 = 2G_f\lambda + (G_m + G_f)(1-\lambda) + (G_f - G_m)\left(\frac{\rho_2^2}{\rho_1^2} - \frac{\rho_1^2}{\rho_2^2}\right)\Big/\left(\rho_2^2 - \frac{1}{\rho_2^2}\right) \tag{53}$$

Substitution of eqns (45) and (50) into eqn (6) yields

$$\frac{I_3}{I_1 G_e + I_2 G_m} + \frac{I_6}{I_4 G_e + I_5 G_m} = \frac{1}{G_m} \tag{54}$$

Eqn (54) can be transformed into a quadratic equation in G_e:

$$I_1 I_4 G_e^2 + (I_1 I_5 + I_2 I_4 - I_3 I_4 - I_6 I_1) G_m G_e + (I_2 I_5 - I_3 I_5 - I_2 I_6) G_m^2 = 0 \tag{55}$$

For a practical composite, G_e has a positive solution and a negative one from eqn (55). Deleting the unreasonable negative solution, we obtain the closed form solution of the effective longitudinal shear modulus G_e:

$$G_e = (-B + \sqrt{B^2 - 4C})G_m/2 \tag{56}$$

where

$$B = (I_1 I_5 + I_2 I_4 - I_3 I_4 - I_6 I_1)/(I_1 I_4) \tag{57}$$

$$C = (I_2 I_5 - I_3 I_5 - I_2 I_6)/(I_1 I_4) \tag{58}$$

4. RESULT COMPARISON AND CONCLUSION

It is of interest to see how the shape of the fiber cross section would affect the effective longitudinal shear modulus of a composite. First, we use the properties of boron fibers and epoxy matrix (Whitney and Riley, 1966) in our calculation. The elastic constants are

Table 1. Variation of the longitudinal shear modulus vs ratio aspect γ

	Longitudinal shear modulus (GPa)									
λ	$\gamma = 1$*	0.9	0.8	0.7	0.6	0.5	0.4	0.2	0.1	0.0001
0.20	2.28	2.28	2.29	2.31	2.35	2.42	2.53	3.32	5.62	35.4
0.50	4.49	4.50	4.57	4.70	4.93	5.34	6.10	11.6	25.0	86.5
0.70	8.28	8.32	8.50	8.87	9.52	10.7	12.8	26.7	50.4	121
0.75	10.1	10.2	10.4	10.9	11.8	13.3	16.1	33.1	59.1	129

* For $\gamma = 1$, the longitudinal shear modulus cannot be directly computed by using the present formula. Instead, γ is taken as a value approaching 1, for example $\gamma = 0.9999$.

$$E_f = 413.69\,\text{GPa}, \quad G_f = 172.37\,\text{GPa}, \quad \nu_f = 0.2$$
$$E_m = 4.1369\,\text{GPa}, \quad G_m = 1.5322\,\text{GPa}, \quad \nu_m = 0.35$$

The longitudinal shear modulus from the present theoretical formula [eqn (56)] for various fiber section aspect ratio γ ($\gamma = b_1/a_1$) are shown in Table 1. It can be seen that the longitudinal shear modulus is very sensitive to the aspect ratio. As the aspect ratio decreases (noting that $0 < \gamma \leqslant 1$ without loss of generality), the longitudinal shear modulus increases for a certain fiber volume fraction. From Fig. 5 in Whitney and Riley (1966) it is seen that the shape of fiber section of the specimens are irregular, so it is improper to be regarded as a circle. To account for the influence of the shape, the fiber sections are taken as an ellipse with $\gamma = 0.4$ and the results are listed in Table 2, which shows that the theoretical predictions are in reasonable agreement with the experimental results.

The second example is the glass-epoxy composite, with the elastic constants being (Zhao and Weng, 1990):

$$E_f = 72.4\,\text{GPa}, \quad G_f = 30.2\,\text{GPa}, \quad \nu_f = 0.2$$
$$E_m = 2.76\,\text{GPa}, \quad G_m = 1.02\,\text{GPa}, \quad \nu_m = 0.35$$

By using the present formula, the normalized longitudinal shear modulus as a function of λ is depicted in Fig. 3. A comparison with the numerical results (Zhao and Weng, 1990) by using Eshelby–Mori–Tanaka theory shows that the results of the two methods are in good agreement.

The present formula is applicable to the whole spectrum of inclusion types, i.e. from voids to rigid inclusions. When the elastic modulus of fibers are equal to zero, the present formula gives the results for materials with voids. The normalized shear modulus predictions for the material with voids are depicted in Fig. 4, which shows that the shear modulus is also very sensitive to the aspect ratio of voids.

Based on the above results and comparison we can make the following conclusions:

1. The proposed inclusion/matrix/composite model of a combined confocal elliptical cylinder unit cell is applicable to the whole spectrum of inclusion types of inclusions (from

Table 2. A comparison of the theoretical predictions of the longitudinal shear modulus with experimental results

	Longitudinal shear modulus (GPa)		
λ	Classical model[1]	Present model[2]	Experiment[3]
0.70	8.27	12.82	12.21
0.75	10.10	16.06	16.75

[1] Referring to Hashin and Rosen, 1964; Whitney and Riley, 1966.
[2] Taking $\gamma = 0.4$.
[3] Referring to Whitney and Riley, 1966.

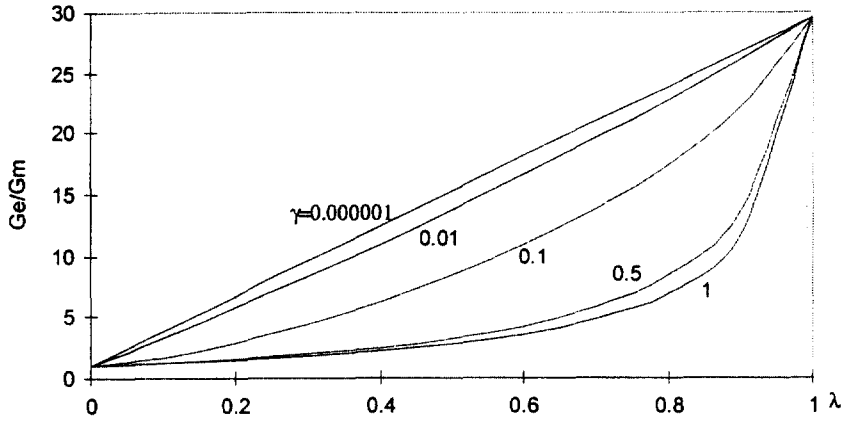

Fig. 3. Variation of the longitudinal shear modulus.

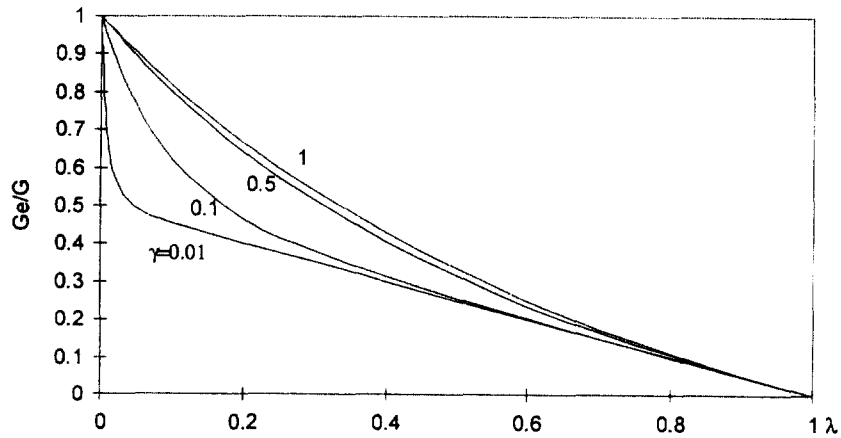

Fig. 4. Shear modulus for the material with voids.

voids to rigid inclusions), and can also accommodate a full range of aspect ratios (from circular fibers to ribbon).

2. By using the conformal mapping technique integrated with the Laurent expansion method, the longitudinal shear modulus is derived in a closed form, which is particularly convenient for application in engineering.
3. A comparison with experimental data and numerical solutions shows the effectiveness and accuracy of the present formula.

The inclusion/matrix/composite model of a combined confocal elliptical cylinder unit cell is also applicable to predict the effective tensile modulus in terms of the other two complex stress functions $\Phi(z)$ and $\Psi(z)$ (Muskhelishivili, 1975); however, it is difficult to obtain the closed form solution. The problem will be dealt with elsewhere.

REFERENCES

Benveniste, Y. (1985) The effective mechanical behavior of composite materials with imperfect contact between the constituents. *Mechanics of Materials* **4**, 197–208.

Christensen, R. M. (1993) Effective properties of composite materials containing voids. *Proceedings of the Royal Society of London* **A440**, 461–473.

Christensen, R. M. and Lo, K. M. (1979) Solutions for effective shear properties in three phase sphere and cylinder models. *Journal of the Mechanics and Physics of Solids* **27**, 315–330.

Hashin, Z. and Rosen, B. W. (1964) The elastic moduli of fiber reinforced materials. *Journal of Applied Mechanics* **31**, 223–232.

Huang, Y. and Hu, K. X. (1995) A generalized self-consistent mechanics method for solids containing elliptical inclusions. *ASME Journal of Applied Mechanics* **62**, 566–572.

Luo, H. A. and Weng, G. J. (1987) On Eshelby's inclusion problem in a three-phase spherically concentric solid, and a modification of Mori–Tanaka's method. *Mechanics of Materials* **8**, 347–361.

Mori, T. and Tanaka, K. (1973) Average stress in the matrix and average elastic energy of materials with misfitting inclusions. *Acta Metallurgica* **21**, 571–574.

Muskhelishivili, N. I. (1975) Some basic problems of mathematical theory of elasticity. Noordhoff, Leyden.

Taya, M. and Chou, T. W. (1981) On two kinds of ellipsoidal inhomogeneities in an infinite elastic body: an application to a hybrid composite. *International Journal of Solids and Structures* **17**, 553–563.

Whitney, J. M. and Riley, M. B. (1966) Elastic properties of fiber reinforced composite materials. *AIAA Journal* **4**(9), 1537–1542.

Zhao, Y. H. and Weng, G. H. (1990) Effective elastic moduli of ribbon-reinforced composites. *ASME Journal of Applied Mechanics* **57**, 158–167.